A

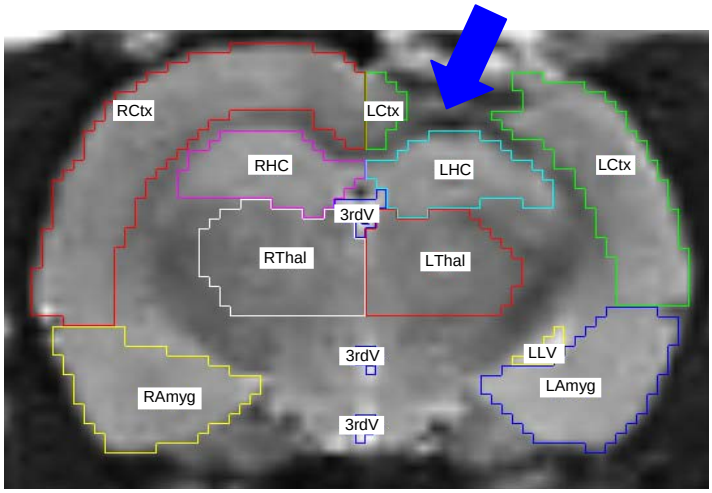
RCtx
LCtx
RHC
LHC
LCtx
3rdV
RThal
LThal
3rdV
LLV
LAmyg
RAmyg
3rdV

B

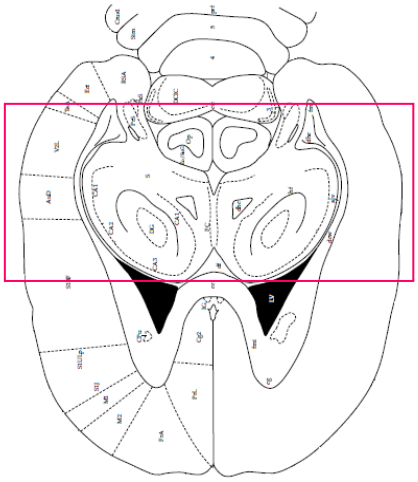

C

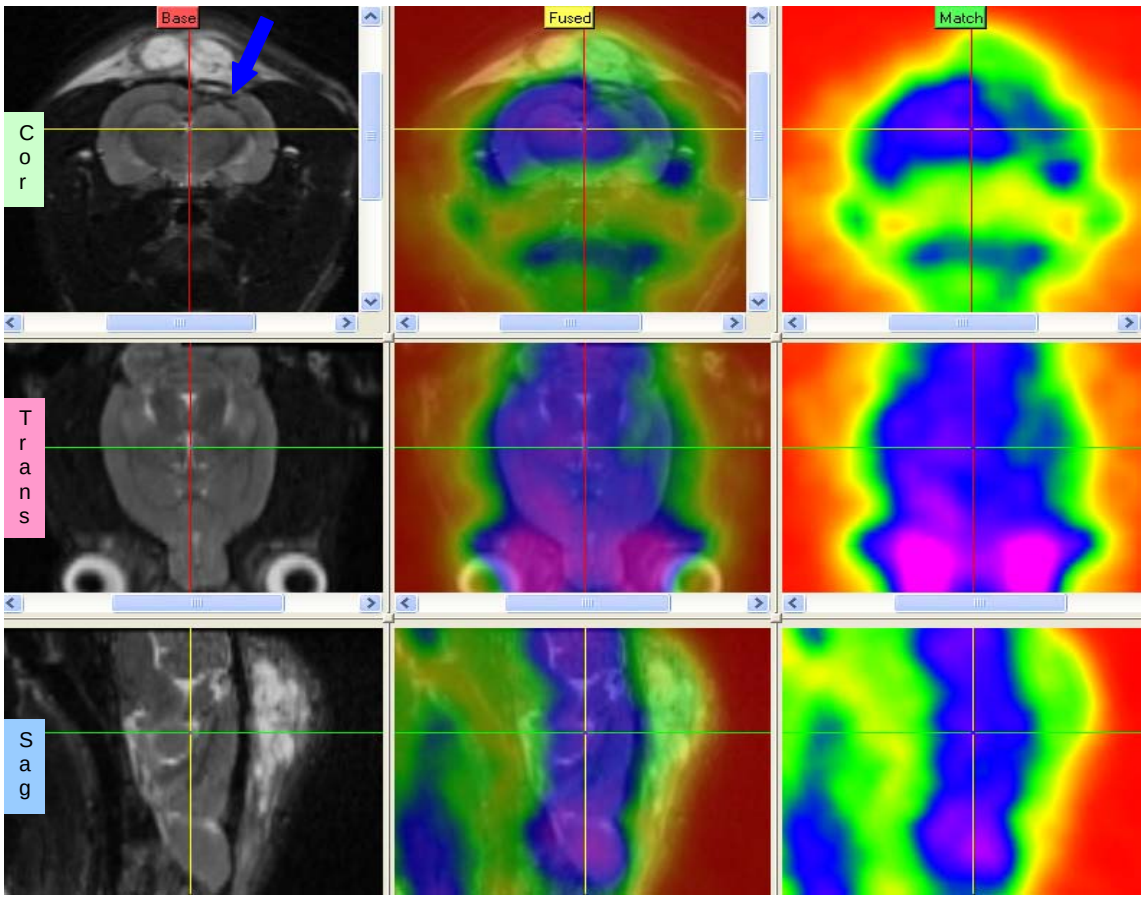
Base
Fused
Match
Cor
Trans
Sag

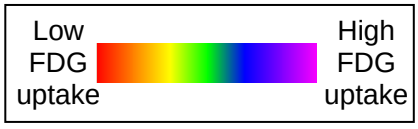
Low
FDG
uptake
High
FDG
uptake

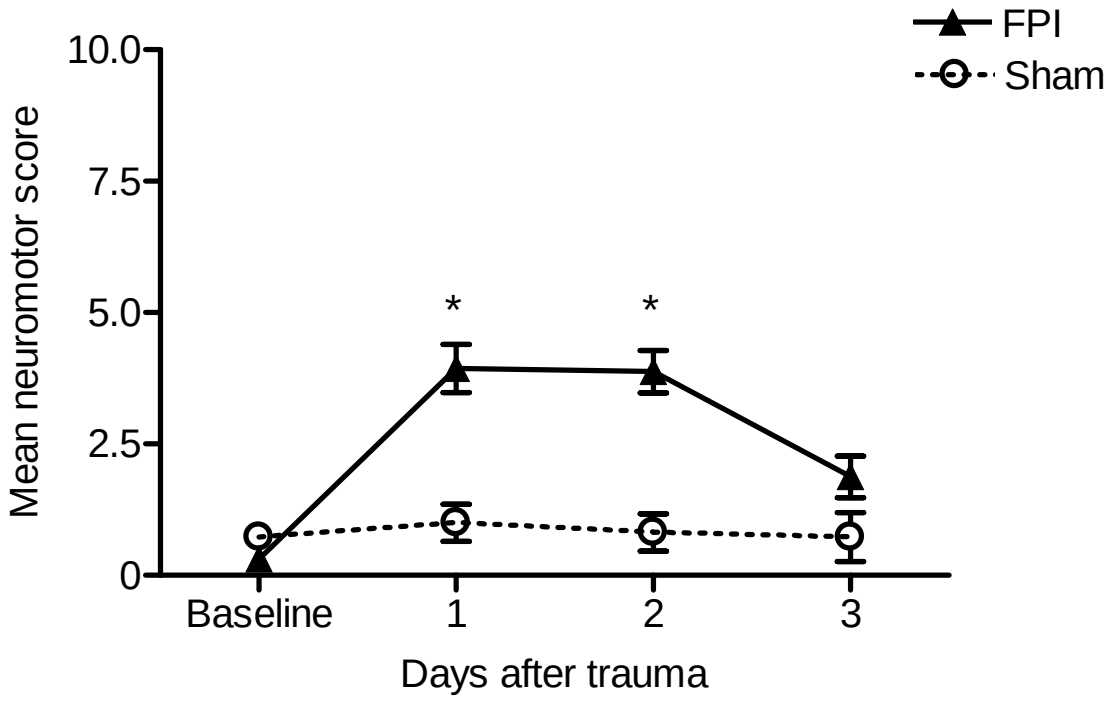
FPI
Sham
Mean neuromotor score
10.0
7.5
5.0
2.5
0
*
*
Baseline
1
2
3
Days after trauma

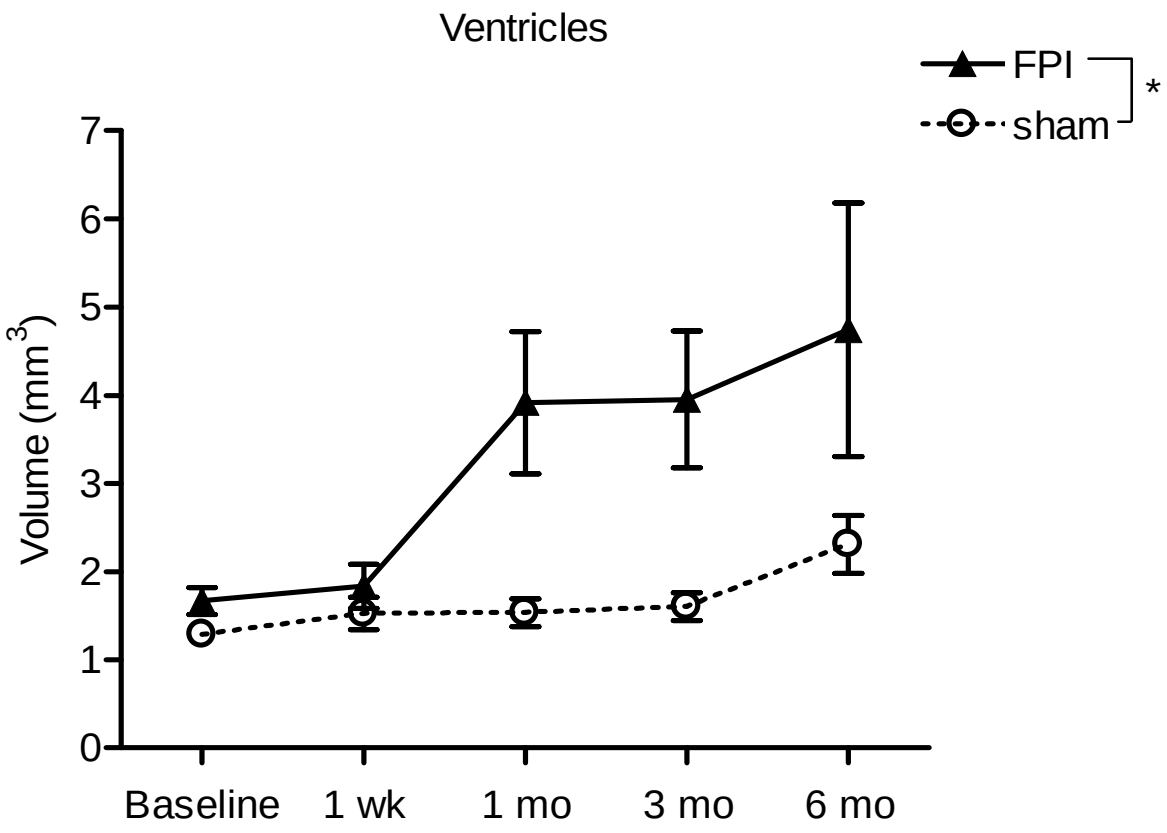
Ventricles
FPI
sham
*
Volume (mm3)
0
1
2
3
4
5
6
7
Baseline
1 wk
1 mo
3 mo
6 mo

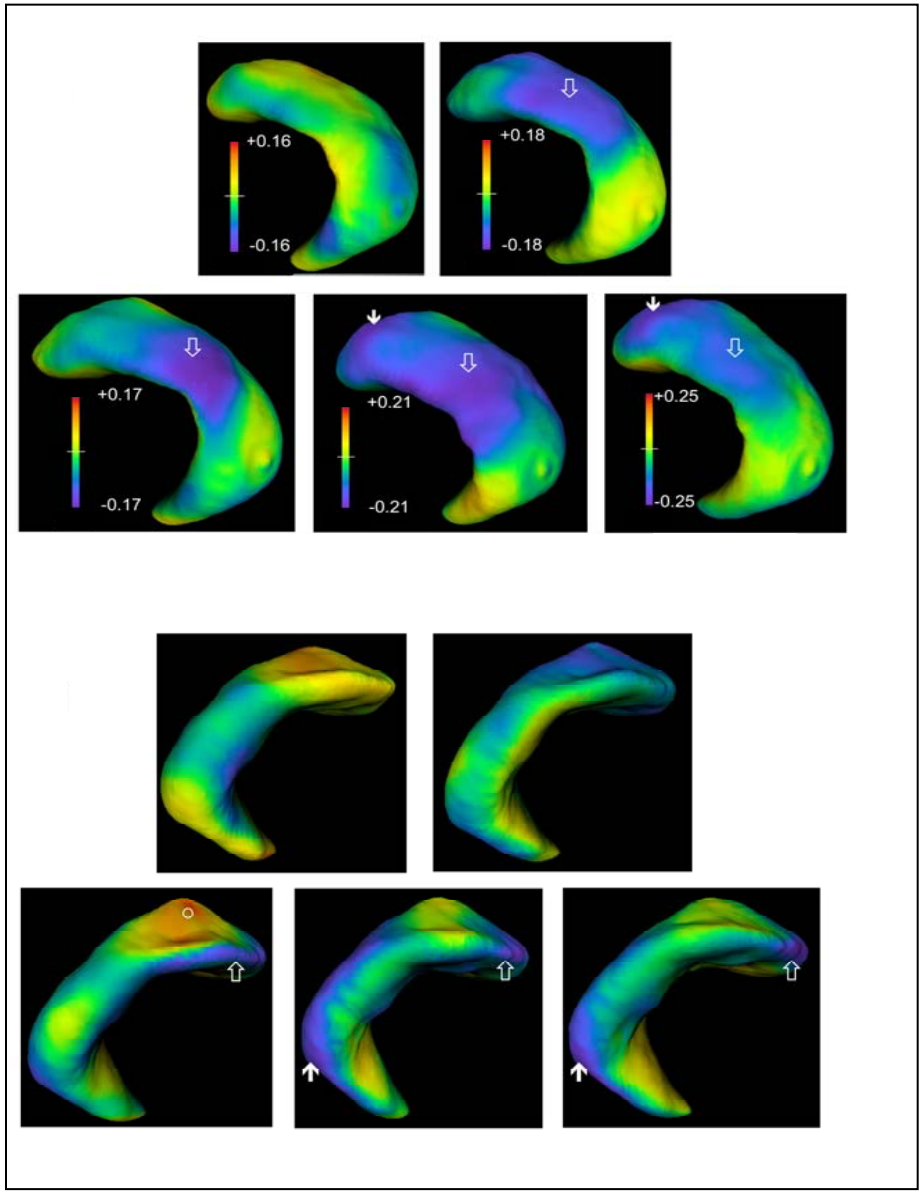
+0.16
-0.16
+0.18
-0.18
+0.17
-0.17
+0.21
-0.21
+0.25
-0.25

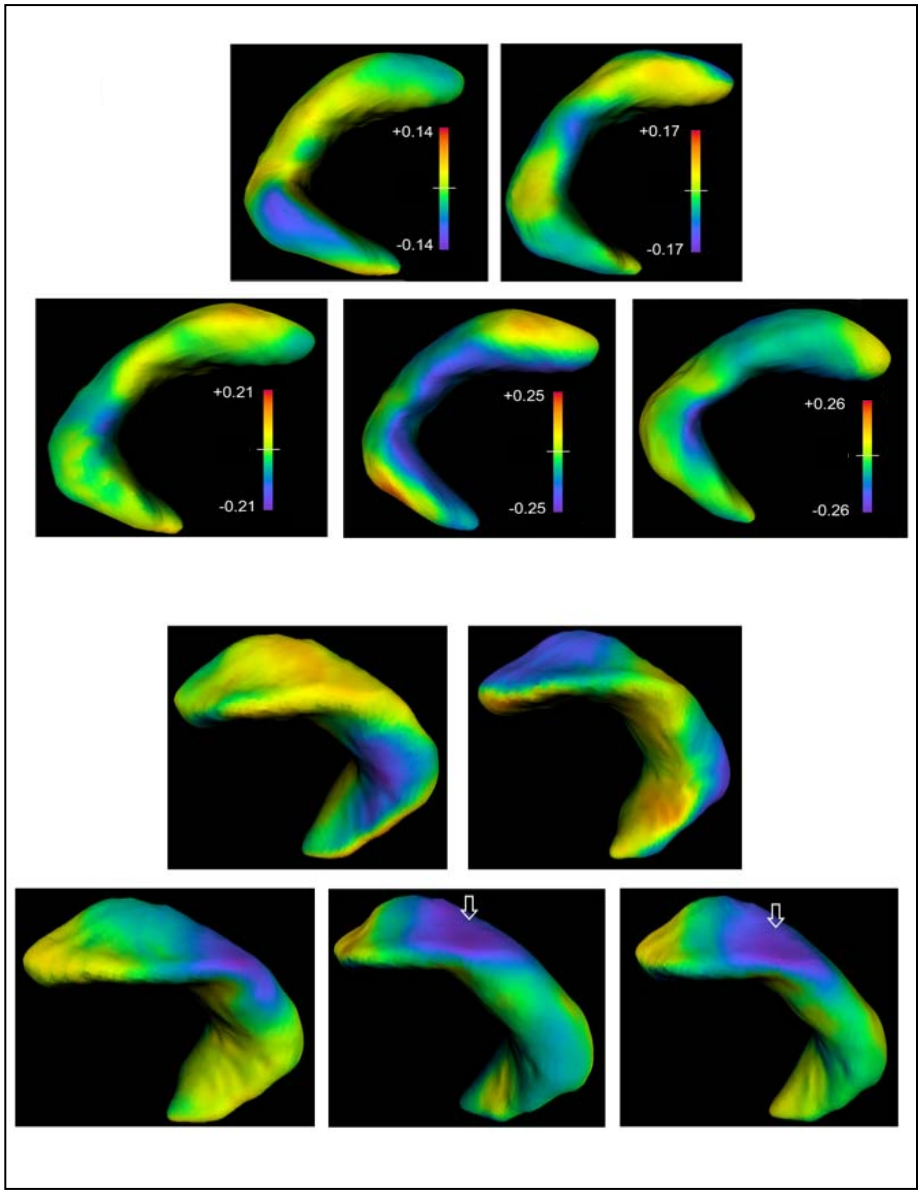
+0.14
-0.14
+0.17
-0.17
+0.21
-0.21
+0.25
-0.25
+0.26
-0.26

Supplemental Figure 5

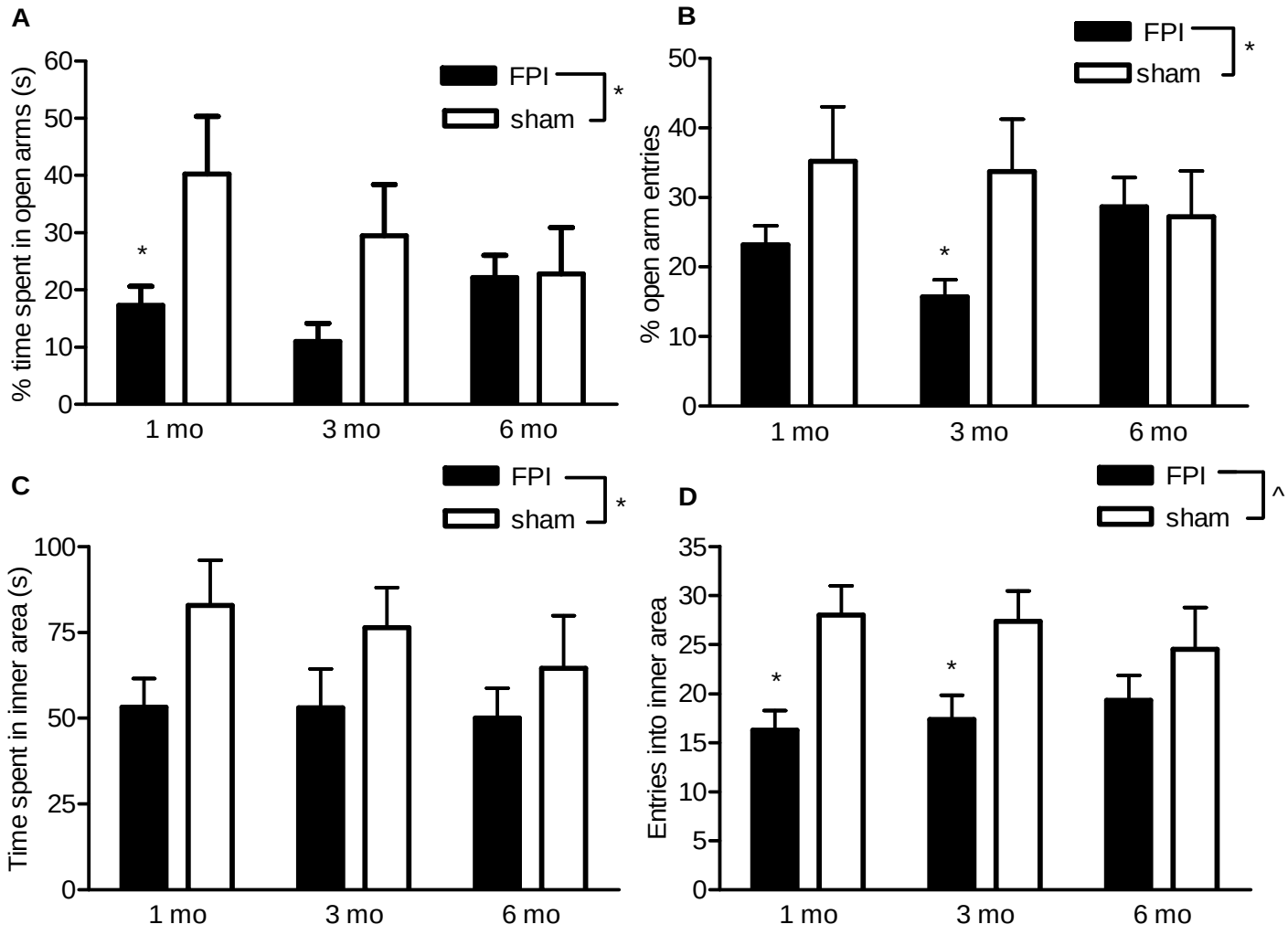

Supplemental Figure 1: (A) The ROIs on MRI, including cortex (Ctx), hippocampus (HC), amygdala (Amyg), thalamus (Thal), the third ventricle (3rd V), and the lateral ventricle (LV). The blue arrow shows the site of the trauma, and the resultant lesion 1 month post-injury. (B) Is a horizontal view of the brain where the ROIs are drawn. (C) PET/MRI co-registration from a representative animal one week post FPI. Note the site of injury (solid blue arrow) and corresponding hypometabolism (open arrow). Cor, coronal section; Sag, sagittal section; Tran, transverse section.

Supplemental Figure 2: Fluid-percussion injury (FPI, triangle, n=16) caused an acute neurological deficit for up to 3 days after impact. Data is expressed as composite neuromotor score (*$p<0.001$); sham-injured animals (circle, n=11) display no deficit; mean±SEM.

Supplemental Figure 3: Progressive cerebral damage post-FPI assessed using MRI, showing the time course of volume changes from baseline in the ventricles, *$p<0.05$; mean±SEM.

Supplemental Figure 4: HDM-LD deformation differences in the hippocampi between FPI and sham rats from the serial MRI scans. Supplemental Figure 4A is the same as Figure 4 in the manuscript, displayed again here to give a better overview of the changes in hippocampal shape. Figures A and B show the regional deformation distances for the left hippocampi (ipsilateral to the injury), with (A) showing a lateral and slightly caudal view and (B) a medial view. Figures C and D show the regional deformation differences

for the right hippocampi, with (C) showing a lateral view and (D) a medial view. Figure A is labelled to show the deformations from the baseline, 1 week, 1 month, 3 month, and 6 month scans. Figures B, C and D are arranged similarly with respect to time after FPI. The open arrows in (A) show a region of inward deformation primarily representing CA2, which becomes visible at one week, progresses at 1 and 3 months, and become less prominent at 6 months. Additionally, the closed arrow (A) at 3 and 6 months shows a region of accentuated volume loss primarily representing CA1. In (B), the open arrows outline progressive changes in CA1 and dentate gyrus regions near the septal pole which evolve from 1 to 6 months. The most caudal region of the hippocampus in (B) is marked by a closed arrow, which also represents CA1 and dentate gyrus regions. A region of outward deformation is marked by an open circle on the 1 month image, and likely represents hippocampal positional shift due to adjacent cortical volume loss. (C) also shows regions of deformation which evolve over time, and differ from the changes on the contralateral side as depicted in (A). In (D) open arrows represent a region of focal deformation change, most prominent at 3 and 6 months, in a region which primarily represents CA1, and differs in distribution as compared to changes in the contralateral hippocampus, as depicted (B).

Supplemental Figure 5: FPI rats (closed bars, n=16) were more anxious than sham rats (open bars, n=11) as shown by less time spent (A) and number of entries (B) into the open arms of the elevated plus maze and significantly less time (C) and less entries (D) into the inner area of the open field; *$p<0.05$, ^$p<0.0005$; mean±SEM.